Journal of Applied Mechanics Vol.9, pp.821-832 (August 2006) JSCE

Approximate Solution for an Axisymmetric Swirling Jet Using Non-Linear k-ε Model with Consideration of Realizability

Md. Shahjahan Ali *, Takashi Hosoda **, Ichiro Kimura***, and Shinichiro Onda****

* PhD Student, Department of Urban Management, Kyoto University (606-8501, Kyoto)
** Professor, Department of Urban Management, Kyoto University (606-8501, Kyoto)
***Department of Civil Engineering, Matsue National College of Technology, (690-8518, Matsue)
****Research Associate, Department of Urban Management, Kyoto University (606-8501, Kyoto)

Using a realizable non-linear k - ε model, the approximate solutions are derived for the fundamental properties of a swirl jet. The functional forms of velocities and k - ε distributions are assumed as a first approximation. The unknown coefficients in the functional forms are obtained as the functions of the non-linear k - ε model constants by substituting the assumed mathematical expressions into the continuity, momentum and non-linear k - ε equations. The coefficient of eddy viscosity ($=c_\mu$) is determined as a function of strain and rotation parameters to satisfy the realizability. Approximate solutions for the turbulent properties are derived from the non-linear Reynolds stress equation. Neglecting the swirl parameter, the same solution is applied to a round jet without swirl. A well agreed comparison is attained between approximate solutions and previous experimental results.

Key Words: *Swirl jet, non-linear k - ε model, RANS, realizability conditions*

1. Introduction

Due to the circumferential motion of jet, the flow field of a swirling jet is more complex than that of a non-swirling jet. However, this type of flow is observed in many natural geophysical as well as anthropogenic activities. Tornado is an example of natural swirling flow. Since the presence of swirl in a jet changes the geometry, coherent structure, spreading and dilutions of the jet fluid, it is sometimes imparted to the flow to control its development. The practical examples include flows through combustors, propulsion devices, cyclone separators etc. Swirl jet can also be used in any environmental mixing devices, where a faster spreading or rapid mixing of jet fluid is necessary.

Most of the previous experimental as well as computational works on swirl jet mainly focused on the region close to the source. Examples are the experimental investigations conducted by Panda and Mclaughin[1], Billant et al.[2], Ribeiro and Whitelaw[3] as well as Paschereit et al.[4], where the interaction of coherent structures of swirl jet just downstream of the nozzle was the main concern. On the other hand, Pratte and Keffer[5] performed the experiments to study the turbulent field of the jet up to a well downstream distance of 30 jet diameters. Although some numerical studies have been performed on near nozzle region of turbulent swirling flows using Reynolds stress model (e. g. Gibson and Younis[6]) and Large eddy simulation (e.g. Mcllwain and Pollard[7], Wang et al.[8]), to the best of our knowledge, the k - ε model is yet to be applied successfully.

Among the turbulence models, k – ε eddy viscosity model is the simplest 'complete' model that can be used on modern personal computers. Due to its simplicity, it became one of the most popular model and found to be adopted frequently. This is a two equation model obtained by solving the turbulent kinetic energy (k) and its dissipation rate (ε) from two differential transport equations. Although this type of model has been applied for prediction of many turbulent flows with high degree of success, it is unable to predict satisfactorily some fundamental flows containing strong streamline curvature, vortices and rotations[9), 10]. This deficiency of this model is due to the isotropic assumption of eddy viscosity that causes mostly a linear relationship between stress and strain rate throughout the turbulent flow field. Thus, in this study, a modified non-linear $k-\varepsilon$ model with consideration of some realizability conditions is applied to derive the approximate solutions for fundamental

properties of a circular swirling jet.

The non-linear $k-\varepsilon$ model is a generalized eddy viscosity model, where additional non-linear terms of mean strain rate are added. In other words, it is also a two equation model where two differential equations are solved for k and ε, and the Reynolds stresses are determined from non-linear algebraic equations by generalizing the eddy viscosity model. Yoshizawa[11] introduced such non-linear relation to Reynolds stresses to admit the anisotropy. Generally, in $k-\varepsilon$ model, the value of the coefficient of eddy viscosity (c_μ) is assumed constant throughout the turbulent flow field, that over predicts its value, especially in the case of large rate of strain and rotation. If the strain is sufficiently large, the model may produce negative normal stresses. Thus, in the present study, a functional form is used for the coefficient of eddy viscosity (c_μ) with the strain (S) and rotation (Ω) parameters, that gives a variable c_μ. Considering the Reynolds stresses as a non-linear polynomial function of mean velocity gradient, such functional form for the coefficient of eddy viscosity was firstly introduced by Pope[12], but that was limited to two dimensional flows. Gatski and Spezille[13] further extended it and proposed a new functional form applicable for three dimensional flows. Recently, Kimura and Hosoda[14] verified the modified $k-\varepsilon$ model with the non-linear anisotropy term. They assumed a functional form of c_μ similar to Pope[12], and examined the realizability conditions for different types of 2D basic flow patterns.

In this paper, the approximate solutions are presented for the fundamental properties of a swirl jet such as spreading rate, distribution of turbulence intensities, turbulent shear stress, turbulent kinetic energy etc., derived by using the modified non-linear $k-\varepsilon$ model. The derived approximate solutions are useful to understand the distributions of turbulent characteristics, the sensitivity of model constants to the distributions of turbulent energy among the turbulent normal stresses, the relation between spreading rate and model constants, etc. The assumed functional form of c_μ is a more generalized one in comparison to previous studies. The constrains of this function is determined considering the realizability conditions for a simple shear flow. Neglecting the swirl parameters from the derived solutions, the spreading rate and turbulent properties are also calculated for a round jet without swirl. Tuning the model constants, the derived solutions are compared with the previous experimental results.

2. Non-Linear k - ε Model

2.1 Basic equations

The basic equations in a k - ε model for an incompressible steady flow are as follows.

Continuity equation:

$$\frac{\partial U_i}{\partial x_i} = 0 \tag{1}$$

Momentum equation:

$$\frac{\partial U_j U_i}{\partial x_j} = g_i - \frac{1}{\rho}\frac{\partial P}{\partial x_i} + \frac{\partial}{\partial x_j}\left(-\overline{u_i u_j}\right) + \nu\frac{\partial^2 U_i}{\partial x_j^2} \tag{2}$$

k - equation:

$$\frac{\partial k U_j}{\partial x_j} = -\overline{u_i u_j}\frac{\partial U_i}{\partial x_j} + \frac{\partial}{\partial x_j}\left\{\left(\frac{\nu_t}{\sigma_k}+\nu\right)\frac{\partial k}{\partial x_j}\right\} - \varepsilon \tag{3}$$

ε - equation:

$$\frac{\partial \varepsilon U_j}{\partial x_j} = -c_{\varepsilon 1}\frac{\varepsilon}{k}\overline{u_i u_j}\frac{\partial U_i}{\partial x_j} + \frac{\partial}{\partial x_j}\left\{\left(\frac{\nu_t}{\sigma_\varepsilon}+\nu\right)\frac{\partial \varepsilon}{\partial x_j}\right\} - c_{\varepsilon 2}\frac{\varepsilon^2}{k} \tag{4}$$

Where, x_i : the spatial coordinates, U_i and u_i : the average and turbulent velocities respectively in x_i direction, P : the pressure, ρ : the density of fluid, ν : the molecular dynamic viscosity, k : the averaged turbulent energy, ε : the averaged turbulent energy dissipation rate, ν_t : the eddy viscosity, σ_k, σ_ε, $c_{\varepsilon 1}$, $c_{\varepsilon 2}$: the model constants (σ_k= 1.0, σ_ε= 1.0, $c_{\varepsilon 1}$ = 1.44 and $c_{\varepsilon 2}$ = 1.92 are used).

To obtain the basic equations of turbulent shear flows, the following assumptions are made[9]:

a) The pressure gradient is small i.e. $\frac{\partial P}{\partial x} \approx 0$

b) Viscous shear stress is much smaller than the turbulent shear stress, and can be neglected.

c) Diffusion in the direction normal to the flow (y- and z-coordinates) is much larger than the diffusion in the direction of flow (x-coordinate).

Thus, the momentum equation in x-direction as well as the k and ε equations can be presented in a simplified form as follows.

The momentum equation in x-direction:

$$U_x\frac{\partial U_x}{\partial x} + U_y\frac{\partial U_x}{\partial y} + U_z\frac{\partial U_x}{\partial z} = \frac{\partial}{\partial x}\left(-\overline{u_x u_x}\right) + \frac{\partial}{\partial y}\left(-\overline{u_x u_y}\right) + \frac{\partial}{\partial z}\left(-\overline{u_x u_z}\right) \tag{5}$$

k - equation:

$$U_x\frac{\partial k}{\partial x} + U_y\frac{\partial k}{\partial y} + U_z\frac{\partial k}{\partial z} = -\overline{u_x u_x}\frac{\partial U_x}{\partial x} - \overline{u_x u_y}\frac{\partial U_x}{\partial y} - \overline{u_x u_z}\frac{\partial U_x}{\partial z}$$

$$-\overline{u_y u_x}\frac{\partial U_y}{\partial x} - \overline{u_y u_y}\frac{\partial U_y}{\partial y} - \overline{u_y u_z}\frac{\partial U_y}{\partial z} - \overline{u_z u_x}\frac{\partial U_z}{\partial x} - \overline{u_z u_y}\frac{\partial U_z}{\partial y}$$

$$-\overline{u_z u_z}\frac{\partial U_z}{\partial z} + \frac{\partial}{\partial y}\left(\frac{\nu_t}{\sigma_k}\frac{\partial k}{\partial y}\right) + \frac{\partial}{\partial z}\left(\frac{\nu_t}{\sigma_k}\frac{\partial k}{\partial z}\right) - \varepsilon \tag{6}$$

ε - equation:

$$U_x\frac{\partial \varepsilon}{\partial x}+U_y\frac{\partial \varepsilon}{\partial y}+U_z\frac{\partial \varepsilon}{\partial z}=c_{\varepsilon 1}\frac{\varepsilon}{k}\Bigg[-\overline{u_x u_x}\frac{\partial U_x}{\partial x}-\overline{u_x u_y}\frac{\partial U_x}{\partial y}$$

$$-\overline{u_x u_z}\frac{\partial U_x}{\partial z}-\overline{u_y u_x}\frac{\partial U_y}{\partial x}-\overline{u_y u_y}\frac{\partial U_y}{\partial y}-\overline{u_y u_z}\frac{\partial U_y}{\partial z}$$

$$-\overline{u_z u_x}\frac{\partial U_z}{\partial x}-\overline{u_z u_y}\frac{\partial U_z}{\partial y}-\overline{u_z u_z}\frac{\partial U_z}{\partial z}\Bigg]$$

$$+\frac{\partial}{\partial y}\left(\frac{\nu_t}{\sigma_\varepsilon}\frac{\partial k}{\partial y}\right)+\frac{\partial}{\partial z}\left(\frac{\nu_t}{\sigma_\varepsilon}\frac{\partial k}{\partial z}\right)-c_{\varepsilon 2}\frac{\varepsilon^2}{k} \qquad (7)$$

2.2 Constitutive equations

In the standard $k-\varepsilon$ model, the Reynolds stress tensor $-\overline{u_i u_j}$ is solved by linear constitutive equations derived from Boussinesq eddy viscosity concept, which does not take into account the anisotropy effect.

$$-\overline{u_i u_j}=\nu_t S_{ij}-\frac{2}{3}k\delta_{ij},\quad S_{ij}=\frac{\partial U_i}{\partial x_j}+\frac{\partial U_j}{\partial x_i} \qquad (8)$$

Here, ν_t is determined from the dimensional consideration of k and ε, and approximated by

$$\nu_t=c_\mu\frac{k^2}{\varepsilon}\quad . \qquad (9)$$

Including the non-linear anisotropy term in the Reynolds stress equation introduced by Yoshizawa[11], the constitutive equations can be expressed in the following forms

$$-\overline{u_i u_j}=\nu_t S_{ij}-\frac{2}{3}k\delta_{ij}-\frac{k}{\varepsilon}\nu_t\sum_{\beta=1}^{3}c_\beta\left(S_{\beta ij}-\frac{1}{3}S_{\beta\alpha\alpha}\delta_{ij}\right) \qquad (10)$$

Here, c_β is the coefficient of non-linear quadratic term; and $S_{\beta ij}$ are defined as :

$$S_{1ij}=\frac{\partial U_i}{\partial x_\gamma}\frac{\partial U_j}{\partial x_\gamma},\quad S_{2ij}=\frac{1}{2}\left(\frac{\partial U_\gamma}{\partial x_i}\frac{\partial U_j}{\partial x_\gamma}+\frac{\partial U_\gamma}{\partial x_j}\frac{\partial U_i}{\partial x_\gamma}\right),$$

$$\text{and}\quad S_{3ij}=\frac{\partial U_\gamma}{\partial x_i}\frac{\partial U_\gamma}{\partial x_j}. \qquad (11)$$

It is known that the non-linear terms in equation (10) are equivalent to the following mathematical formulation[11), 13)].

$$\alpha_1(S_{il}\Omega_{lj}+\Omega_{li}S_{jl})+\alpha_2(S_{il}S_{lj}-\frac{1}{3}S_{km}S_{mk}\delta_{ij})$$

$$+\alpha_3(\Omega_{il}\Omega_{lj}-\frac{1}{3}\Omega_{km}\Omega_{mk}\delta_{ij}) \qquad (12)$$

Where, the strain and rotation tensors are defined as

$$S_{ij}=\frac{\partial U_i}{\partial x_j}+\frac{\partial U_j}{\partial x_i},\quad \Omega_{ij}=\frac{\partial U_i}{\partial x_j}-\frac{\partial U_j}{\partial x_i} \qquad (13)$$

Comparing Eq. (12) with the non-linear terms of Eq. (10), the relations between the coefficients can be derived as

$$c_1=-2\alpha_1+\alpha_2-\alpha_3,\ c_2=2(\alpha_2+\alpha_3),\ c_3=2\alpha_1+\alpha_2-\alpha_3 \qquad (14)$$

From this comparison, it is also inferred that the coefficient of eddy viscosity (c_μ) is the function of strain and rotation parameters. The strain parameter (S) and rotation parameter (Ω) are defined in Eq. (15), as used in the previous studies of Pope[12], and Gatski and Speziale[13].

$$S=\frac{k}{\varepsilon}\sqrt{\frac{1}{2}S_{ij}S_{ij}},\quad \Omega=\frac{k}{\varepsilon}\sqrt{\frac{1}{2}\Omega_{ij}\Omega_{ij}} \qquad (15)$$

In this study, the assumed form of c_μ is more generalized than previous one, that can be expressed as

$$c_\mu=\frac{c_{\mu o}(1+c_{ns}S^2+c_{n\Omega}\Omega^2)}{1+c_{ds}S^2+c_{d\Omega}\Omega^2+c_{ds\Omega}S\Omega+c_{ds1}S^4+c_{d\Omega 1}\Omega^4+c_{ds\Omega 1}S^2\Omega^2} \qquad (16)$$

Here, $c_{\mu 0}$, c_{ns}, $c_{n\Omega}$, c_{ds}, $c_{d\Omega}$, $c_{ds\Omega}$, c_{ds1}, $c_{d\Omega 1}$, and $c_{ds\Omega 1}$ are the model constants. The functional form assumed by Gatski and Speziale[13] can be obtained from the above equation simply neglecting some higher order terms i.e. substituting $c_{n\Omega}$, $c_{ds\Omega}$, c_{ds1}, and $c_{d\Omega 1}$ as zero. The more simplified functional form of c_μ, suggested by Pope[12] for two dimensional flows, can be obtained neglecting some more terms from the above equation.

Assuming a similar functional form for c_β, Kimura and Hosoda[14] compared the analytical results for diagonal components of the anisotropic tensor with that of experiments for simple shear flows. They showed that the assumed functional form for the coefficient of quadratic term c_β, gave better results instead of taking their constant values. In this analysis, the following functional form is assumed for c_β.

$$c_\beta=c_{\beta o}\frac{1+m_{ns}S^2+m_{n\Omega}\Omega^2}{1+m_{ds}S^2+m_{d\Omega}\Omega^2} \qquad (17)$$

Where, m_{ns}, $m_{n\Omega}$, m_{ds}, and $m_{d\Omega}$ are the model constants.

3. Procedure for the Solution

Firstly, the functional forms of velocities and $k-\varepsilon$ distributions are assumed as a first approximation. Using the integral equation of momentum conservation, the parameter accounted for swirl (introduced in velocity distributions) is derived as function of non-dimensional swirl number, S_N. Substituting the mathematical expressions of the assumed distributions into the continuity, momentum and non-linear $k-\varepsilon$ equations, a set of algebraic equations are derived considering the relation of lowest order with respect to the power of (1/x). Solving these simultaneous algebraic equations, the unknown coefficients in the assumed

distributions are determined as the function of the non-linear $k-\varepsilon$ model constants. Approximate solutions for the distributions of turbulence characteristics such as distribution of turbulence intensities, turbulent shear stress, etc. are derived using the constitutive equations of the model.

The coefficients in the functional forms of c_μ and c_β are initially estimated considering realizability conditions for plane shear layer. Neglecting the swirl parameters, the derived solutions for swirl jet are applied for a round jet without swirl. The results are compared with the previous experiments, and the model constants are finally determined by tuning their values for best fitting with the previous results. The fundamental properties of swirl jet are then predicted using the same model constants, and compared with the previous experimental data.

4. Consideration of Realizability

4.1 Realizability inequalities

Realizability can be defined as the requirement of the non-negativity of turbulent normal stresses and Schwarz' inequality between any turbulent velocity correlations.[14] It is a basic physical and mathematical principle that the solution of any turbulence model equation should obey.[15] The realizability inequalities for 3D turbulent flows are:

$$\overline{u_i u_i} \geq 0 \tag{18a}$$

$$\overline{u_i u_i} \cdot \overline{u_j u_j} \geq \overline{u_i u_j}^2 \quad (i \neq j) \tag{18b}$$

$$\det \begin{bmatrix} \overline{u_1 u_1} & \overline{u_1 u_2} & \overline{u_1 u_3} \\ \overline{u_2 u_1} & \overline{u_2 u_2} & \overline{u_2 u_3} \\ \overline{u_3 u_1} & \overline{u_3 u_2} & \overline{u_3 u_3} \end{bmatrix} \geq 0 \tag{18c}$$

Einstein's summation rule is not applied in Eq. (18). In a two dimensional averaged flow, Eq. (18b) coincides with Eq. (18c). In this study, the restrictions on c_μ are derived from the mentioned realizability equations for simple shear flow. The functional forms for c_μ and c_β, as expressed in Eqs. (16) and (17) respectively, are applied in this study.

4.2 Analysis of inequality for simple shear flow

Applying Eq. (18a) to plane shear layer, the following two equations are derived for the diagonal components of the Reynolds stress tensor

$$\frac{\overline{u_1 u_1}}{k} = \frac{2}{3} + \frac{c_\mu (2c_3 - c_1)}{3} M^2 \geq 0 \tag{19a}$$

$$\frac{\overline{u_2 u_2}}{k} = \frac{2}{3} + \frac{c_\mu (2c_3 - c_1)}{3} M^2 \geq 0 \tag{19b}$$

Where, M = maximum (S,Ω); for plane shear layer, $M=S=\Omega$. Applying Eq. (18b), the following inequality equation can be derived for Reynolds stress component, $\overline{u_1 u_2}$.

$$c_\mu^2 \left\{ 9M^2 + (2c_1^2 + 2c_3^2 - 5c_1 c_3) M^4 \right\} - 2c_\mu (c_1 + c_3) M^2 - 4 \leq 0 \tag{19c}$$

Since the value of c_1 is positive and c_3 is negative, Eq. (19a) is satisfied regardless of M. Thus, the restrictions on c_μ, derived from Eqs. (19b) and (19c), are as follows:

$$c_\mu \leq \frac{2}{(c_1 - 2c_3) M^2} \tag{20}$$

$$c_\mu \leq \frac{(c_1 + c_3) M \sqrt{(c_1 + c_3)^2 M^2 + 4\left\{9 + (2c_1^2 + 2c_3^2 - 5c_1 c_3) M^2\right\}}}{9M + (2c_1^2 + 2c_3^2 - 5c_1 c_3) M^3} \tag{21}$$

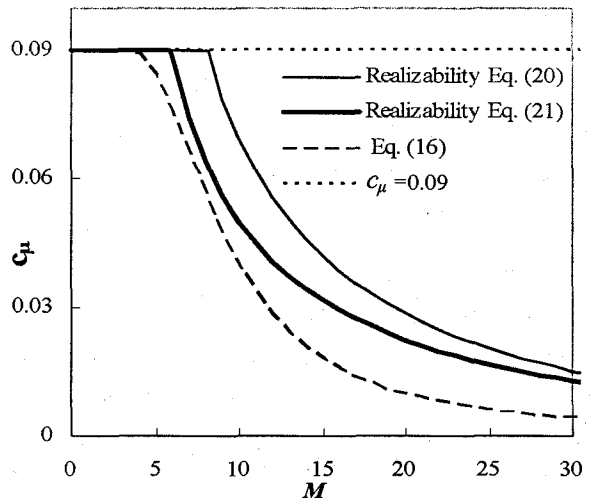

Fig.1 Relation between c_μ and M in a simple shear layer

Following values, for the coefficients of functional forms of c_β, are proposed from our previous studies in flows around bluff bodies:

c_{10} =0.40, c_{20} =0, and c_{30} = -0.13.

For plane shear layer, the realizability conditions [Eqs. (20) and (21)] as well as the proposed functional form of c_μ [Eq. (16)] are plotted in Fig. 1. The calculations are made with the following values of model constants.

$c_{\mu 0}$= 0.09, $c_{ns}+c_{n\Omega}$= 0.014, $c_{ds}+c_{d\Omega}+c_{ds\Omega}$ = 0.009, c_{ds1} $+c_{d\Omega 1}+c_{ds\Omega 1}$= 0.00035, $m_{ns}+m_{n\Omega}$= 0.004, $m_{ds}+m_{d\Omega}$= 0.022 (22)

These values of model constants are initially estimated based on the realizability conditions as derived in Eqs. (20) and (21). Using the estimated values, the approximate solutions are compared with the previous experimental results and the values of model constants are finally determined by tuning their values for best-fitted results.

Eq.(22) shows the final values of constants obtained by such a trial and error method, and Fig. 1 confirms that the model obeys the realizability conditions with these values of constants.

In the log-law region, the assumed functional form of c_μ shows almost a constant value of 0.09. It can be noted that, instead of functional form, if a constant value of c_μ (=0.09) is used through out the turbulent flow field (shown as dotted line in the figure), it fails to satisfy the realizability conditions.

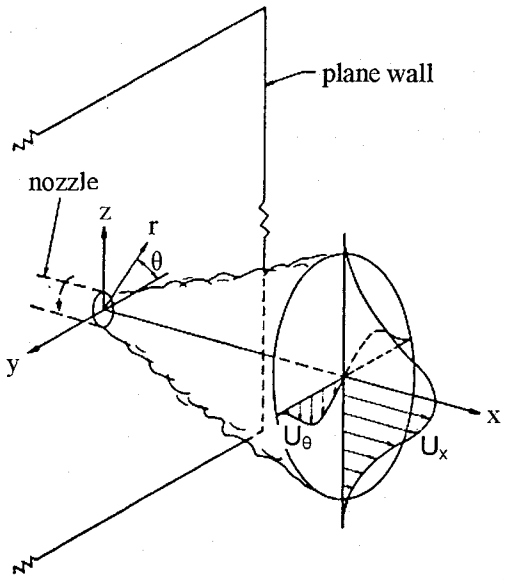

Fig.2 Definition sketch of swirl jet (Pratte and Keffer[5])

5. Derivation of Approximate Solutions

Figure 2 shows the definition sketch of a swirl jet with Cartesian and Cylindrical coordinate systems. Consider, U_x, U_y, and U_z are the jet velocities in axial (x), lateral (y), and transverse (z) directions (in Cartesian coordinate system) respectively. In the self-similar region, the following relations can be obtained for the attenuation rate of hydraulic variables of an axisymmetric swirl jet.[16), 17)]

$$B \propto x, \quad U_m \propto \frac{1}{x}, \quad k_0 \propto \frac{1}{x^2}, \quad \varepsilon_0 \propto \frac{1}{x^4} \tag{23}$$

Here, B is the jet width, U_m is the centerline maximum velocity of the jet, k_0 and ε_0 are the centerline values of turbulent kinetic energy and its dissipation rate respectively.

The following assumptions are made for the functional forms of velocity and $k-\varepsilon$ distributions, which are compatible with the decaying power low of velocity and $k-\varepsilon$ along the centerline of jets.

$$U_x = \frac{a_1}{x}\exp\left(-\frac{y^2+z^2}{\gamma^2x^2}\right)+\frac{a_3}{x}\frac{y^2+z^2}{\gamma^2x^2}\exp\left(-\frac{y^2+z^2}{\gamma^2x^2}\right) \tag{24}$$

$$U_y = \frac{b}{x}\frac{y}{\gamma x}\exp\left(-\frac{y^2+z^2}{\gamma^2x^2}\right)+\frac{\alpha z}{\gamma x^3}\exp\left(-\frac{y^2+z^2}{\gamma^2x^2}\right) \tag{25}$$

$$U_z = \frac{b}{x}\frac{z}{\gamma x}\exp\left(-\frac{y^2+z^2}{\gamma^2x^2}\right)-\frac{\alpha y}{\gamma x^3}\exp\left(-\frac{y^2+z^2}{\gamma^2x^2}\right) \tag{26}$$

$$k = \frac{1}{x^2}\left(k_0+k_2\frac{y^2+z^2}{\gamma^2x^2}\right)\exp\left(-2\frac{y^2+z^2}{\gamma^2x^2}\right) \tag{27}$$

$$\varepsilon = \frac{1}{x^4}\left(\varepsilon_0+\varepsilon_2\frac{y^2+z^2}{\gamma^2x^2}\right)\exp\left(-3\frac{y^2+z^2}{\gamma^2x^2}\right) \tag{28}$$

Where, a_1, a_3, b, α, and γ are the unknown coefficients of the velocity profile, and k_0, k_2, ε_0, and ε_2 are that of the k-ε distributions.

To define the swirl parameter, consider the cylindrical coordinate system, and assume that U_x, U_r, and U_θ are the velocities in axial (x), radial (r), and azimuthal (θ) directions respectively. Rajaratnam[17)] showed that for the circular jet with swirl, integral of the pressure plus momentum (W) as well as angular momentum (T) are preserved. They are defined by

$$W = \int_0^\infty\left(U_x^2-\frac{U_\theta^2}{2}\right)r\,dr \tag{29}$$

and $$T = \int_0^\infty r^2U_xU_\theta\,dr \tag{30}$$

respectively.

Considering $U_x >> U_\theta$, Eq. (29) can be reduced to

$$W = \int_0^\infty U_x^2 r\,dr \tag{31}$$

Substituting the assumed velocity distributions into Eqs. (30) and (31), the following relations are obtained (U_θ is calculated from U_y and U_z).

$$W = \frac{\gamma^2}{8}\left(2a_1^2+2a_1a_3+a_3^2\right) \tag{32}$$

$$T = \frac{\alpha\gamma^3}{8}\left(a_1+a_3\right) \tag{33}$$

Usually, a non-dimensional parameter combining W and T is used to represent the relative amount of swirl in a flow called swirl number (S_N).

$$S_N = \frac{T}{W r_0} \tag{34}$$

where, r_0 is the radius of the jet nozzle.

Using Eqs. (32) to (34), the swirl number can be defined as

$$S_N = \frac{6\alpha\gamma^2}{25br_0} \tag{35}$$

Hence,

$$\alpha = \frac{25S_N br_0}{6\gamma^2} \tag{36}$$

Substituting the assumed velocity distributions [Eqs. (24) to (26)] into the continuity equation, the following algebraic relations are derived.

$$a_1 = \frac{2b}{\gamma}, \quad a_3 = \frac{2}{3}\frac{b}{\gamma} \tag{37-a, b}$$

The integral equation for conservation of momentum flux also results in Eq. (38).

$$M_0 = U_0{}^2 A_0 = 2\pi\left(\frac{a_1^2\gamma^2}{4} + 2\frac{a_1 a_3\gamma^2}{8} + \frac{a_3^2\gamma^2}{8}\right) \tag{38}$$

Where, A_0, U_0, and M_0 are the area, velocity, and initial momentum flux of the jet at inlet respectively.

Substituting Eq. (37) into Eq. (38), the coefficient of attenuation of radial velocity 'b' is determined in Eq. (39) as a function of inlet conditions.

$$b = \frac{3}{5}\sqrt{\frac{M_0}{\pi}} \tag{39}$$

For the assumed velocity and $k-\varepsilon$ distributions, using the Reynolds equation in the x-direction and $k-\varepsilon$ equations, the following three algebraic expressions are derived as the relations of lowest order with respect to the power of $1/x$.

Reynolds equation in x-direction:

$$\frac{1}{x^3}: \quad -a_1^2\left\{\varepsilon_0^2 + \frac{1}{2}c_{ds}k_0^2\left(4a_1^2 + 8\frac{b^2}{\gamma^2}\right)\right\} = 2c_{\mu_0}\varepsilon_0 k_0^2$$

$$\left\{\varepsilon_0{}^2 + \frac{1}{2}c_{ns}\frac{k_0^2}{\varepsilon_0^2}\left(4a_1^2 + 8\frac{b^2}{\gamma^2}\right)\right\}\left(\frac{2a_3}{\gamma^2} - \frac{2a_1}{\gamma^2} - \frac{2b}{\gamma}\right) \tag{40}$$

k-equation:

$$\frac{1}{x^4}: \quad \left(-2a_1k_0 + \varepsilon_0\right)\left\{\varepsilon_0^2 + \frac{1}{2}c_{ds}k_0^2\left(4a_1^2 + 8\frac{b^2}{\gamma^2}\right)\right\}$$

$$= \frac{c_{\mu_0}}{\sigma_k}\varepsilon_0 k_0^2\left(\frac{4k_2}{\gamma^2} - \frac{8k_0}{\gamma^2}\right)\left\{\varepsilon_0^2 + \frac{1}{2}c_{ns}\frac{k_0^2}{\varepsilon_0^2}\left(4a_1^2 + 8\frac{b^2}{\gamma^2}\right)\right\} \tag{41}$$

ε -equation:

$$\frac{1}{x^6}: \quad \left(-4a_1\varepsilon_0 k_0 + c_{\varepsilon 2}\varepsilon_0^2\right)\left\{\varepsilon_0^2 + \frac{1}{2}c_{ds}k_0^2\left(4a_1^2 + 8\frac{b^2}{\gamma^2}\right)\right\}$$

$$= \frac{c_{\mu_0}}{\sigma_\varepsilon}\varepsilon_0 k_0^3\left(\frac{4\varepsilon_2}{\gamma^2} - \frac{8\varepsilon_0}{\gamma^2}\right)\left\{\varepsilon_0^2 + \frac{1}{2}c_{ns}\frac{k_0^2}{\varepsilon_0^2}\left(4a_1^2 + 8\frac{b^2}{\gamma^2}\right)\right\} \tag{42}$$

The values of b, a_1 and a_3 are determined by Eqs. (37) and (39). Substituting the values of k_0 and ε_0 which are the $k-\varepsilon$ values at centerline, the development rate of swirl jet (γ) can be estimated by Eq. (40). For any known value of swirl number S_N, the value of 'α' can be determined using Eq. (36). The coefficients of k and ε distributions are determined by solving the Eqs. (41) and (42).

The radial distributions of turbulent intensities as well as turbulent shear stresses are derived by constitutive equations. The derived equations for turbulent intensities in axial (x), radial (r) and azimuthal (θ) directions, expressed as $\overline{u_x u_x}$, $\overline{u_r u_r}$ and $\overline{u_\theta u_\theta}$ respectively, as well as the component of turbulent shear stress $\overline{u_x u_r}$ are shown in the Appendix -A.

6. Results and Discussion

6.1 Round jet without swirl

Eliminating swirl parameter i.e. taking swirl number (S_N) and hence the swirl parameter (α) as zero, the solutions for swirl jet derived in previous section are applied for a round jet without swirl. Tuning the model constants (estimated from realizability considerations), their values are finally determined for best fitting the approximate solutions with the previous experimental results. Table 1 shows the obtained values for model constants.

The turbulent distributions are calculated with the centerline values of k and ε for round jet as $k_0 = 2.94U_0^2A_0$ and $\varepsilon_0 = 26.33U_0^3A_0^{3/2}$ respectively. Figures 3, 4, and 5 show the radial distributions of turbulent intensities for axial, radial and circumferential velocities. The results are compared with the experimental data by Wygnanski and Fielder[18], and Wang and Law[19]. Figures show an excellent agreement between approximate solutions and measured distributions. In Fig. 6, the calculated shear stress profile is compared with the range of experimental results by Fukushima et al.[20], where two experimental profiles represent the lower and upper boundary of a number of measured profiles for different downstream distances.

Using the approximate solution, the turbulent intensities are also calculated by the standard $k-\varepsilon$ model as shown in the figures by dotted line. Since, the standard k–ε model cannot handle the anisotropic phenomena of turbulence, its prediction is not as good as that of non-linear one. In the analysis of non-linear k–ε model, the value of model constant σ_ε is taken as 1.0 instead of its standard value of 1.3. The comparative predictions are shown in Figs. 3 and 6. Although the difference is very small, in comparison to experimental results, σ_ε=1.0 shows better fitted results than

σ_ε=1.3.

The distribution of turbulent kinetic energy (k) normalized by U_m^2 is favorably compared with the experiment of Wygnanski and Fielder[18], and shown in Fig.7. The normalized turbulent energy dissipate rate ($\varepsilon x/U_m^3$), compared with the experimental data of Wygnanski & Fielder as well as with that of Sami[21], is shown in Fig. 8. The available experimental data on turbulent kinetic energy are quite scattered. The present prediction coincides with the Wygnanski & Fielder's data near the central region of jet and it is close to Sami's data for higher radial distances. In comparison to experimental results, a little deviation is observed in the spreading of k and ε profiles; it can be noted that this deficiency is due to the simple assumptions that made in the exponential part of k and ε distributions [Eqs. (27) and (28)].

Table 1. Values for the coefficients of c_μ and c_β

Model constants	Values for model constants
$c_{\mu 0}$	0.09
c_{ns}	0.006
$c_{n\Omega}$	0.008
c_{ds}	0.008
$c_{d\Omega}$	0.004
$c_{ds\Omega}$	-0.003
c_{ds1}	0.00005
$c_{d\Omega 1}$	0.00005
$c_{ds\Omega 1}$	0.00025
m_{ns}	0.002
$m_{n\Omega}$	0.002
m_{ds}	0.03
$m_{d\Omega}$	-0.008

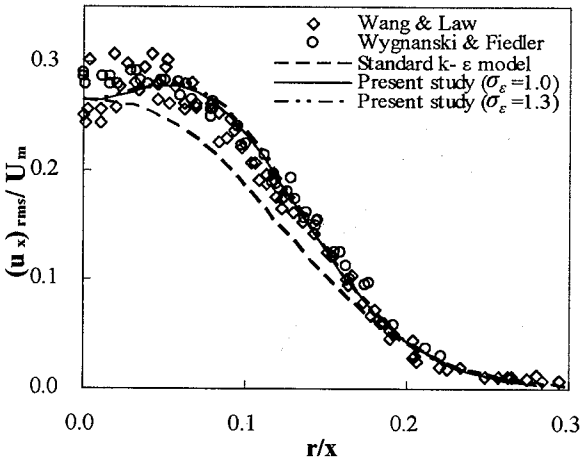

Fig.3 Distribution of turbulent intensity of the axial velocity in a round jet without swirl

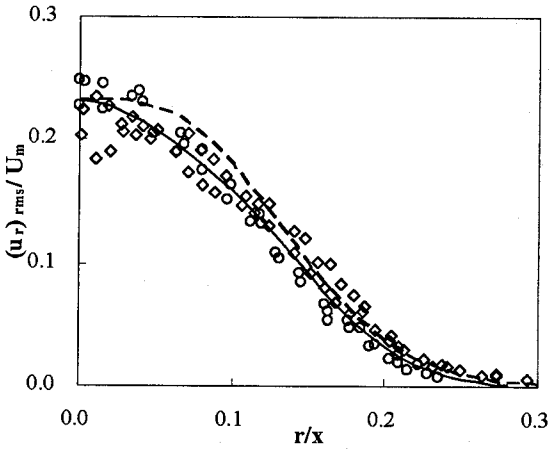

Fig.4 Distribution of turbulent intensity of the radial velocity in a round jet without swirl

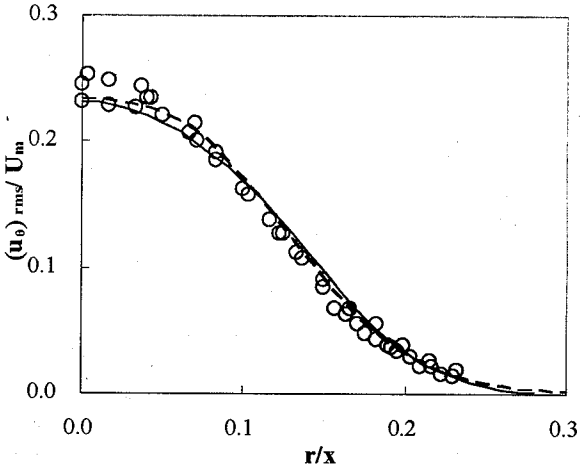

Fig.5 Distribution of turbulent intensity of the circumferential velocity in a round jet without swirl

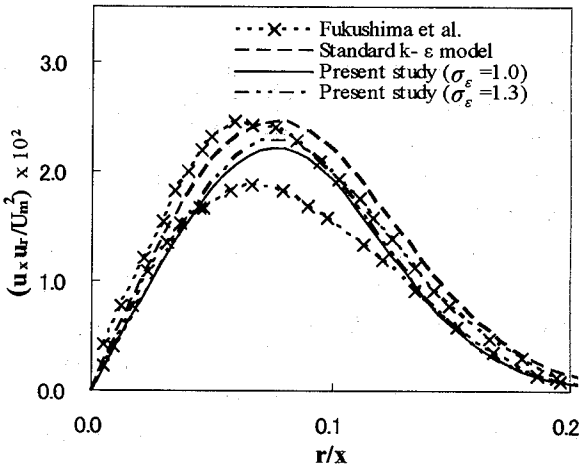

Fig.6 Radial distribution of turbulent shear stress in a round jet without swirl

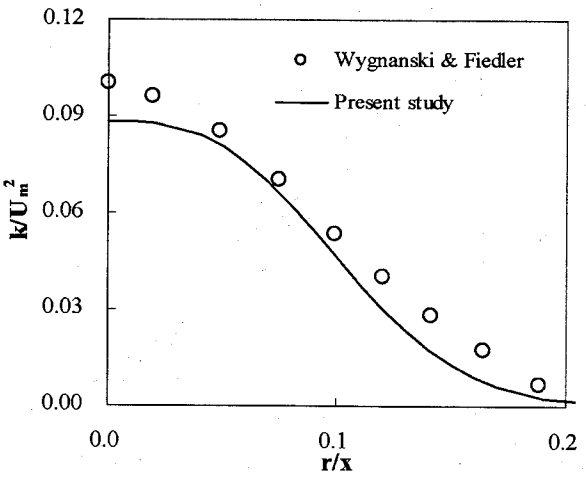

Fig.7 Radial distribution of turbulent kinetic energy in a round jet without swirl

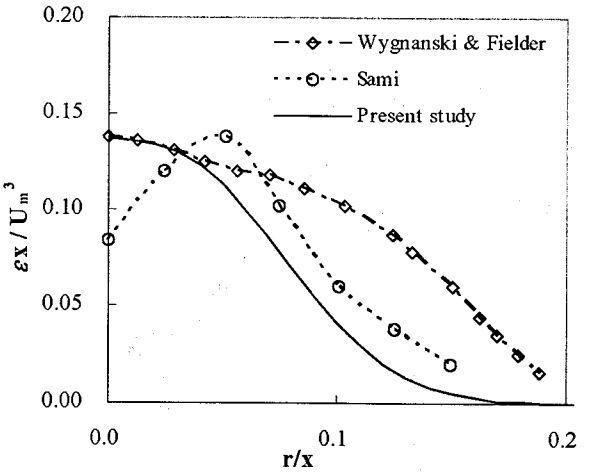

Fig.8 Radial distribution of turbulent kinetic energy dissipation rate in a round jet without swirl

6.2 Swirl jet

Using the model constants estimated in Table 1, and taking estimated centerline values of k and ε for swirl jet as $k_0=2.0U_0^2A_0$ and $\varepsilon_0=10.2U_0^3A_0^{3/2}$ respectively, the fundamental properties of a swirl jet are obtained and presented below.

In Fig. 9, the estimated jet half-width for a moderate swirl of S_N =0.3 is plotted against downstream distances; both are normalized with initial jet diameter D. Here, the jet half-width ($r_{1/2}$) is defined as the radial distance (r), where the axial velocity is half of the maximum centerline velocity. The present prediction shows a good agreement with the previous experimental data of Pratte and Keffer[5] (S_N=0.3) as well as that of Rose[22] (S_N=0.23). The prediction of Reynolds Stress Model (RSM) by Gibson and Younis[6], which is limited to 15 jet diameters of downstream distances, are also shown for comparison. The swirl jet reasonably spreads faster than the round jet. The value of jet half-width for swirl jet evaluated by approximate solution is 0.144,

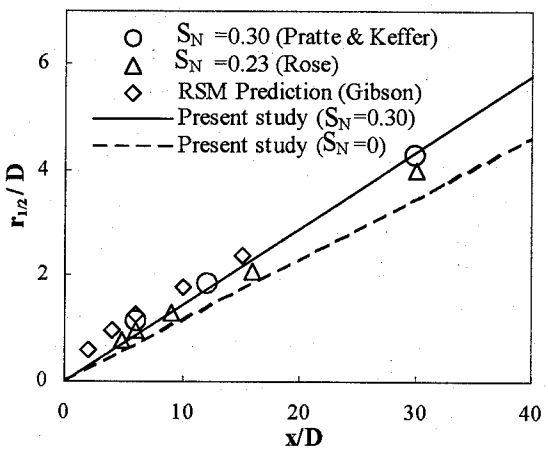

Fig.9 Comparison of jet half-width

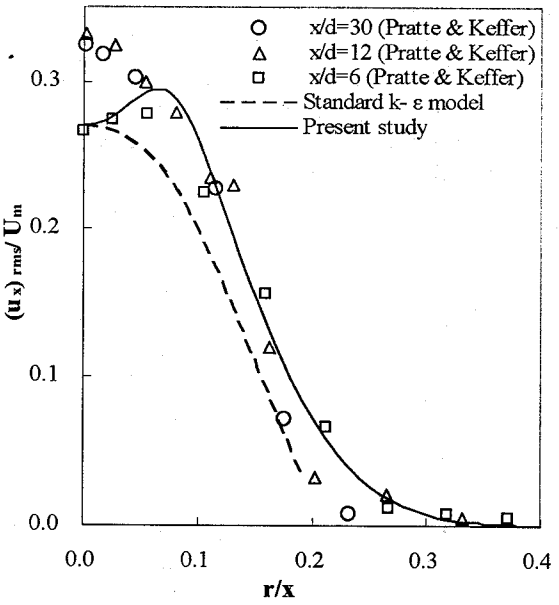

Fig.10 Distribution of turbulent intensity of the axial velocity in a swirl jet

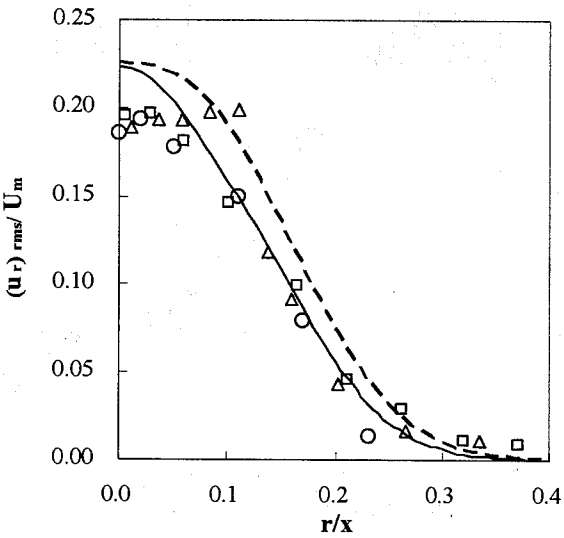

Fig.11 Distribution of turbulent intensity of the radial velocity in a swirl jet

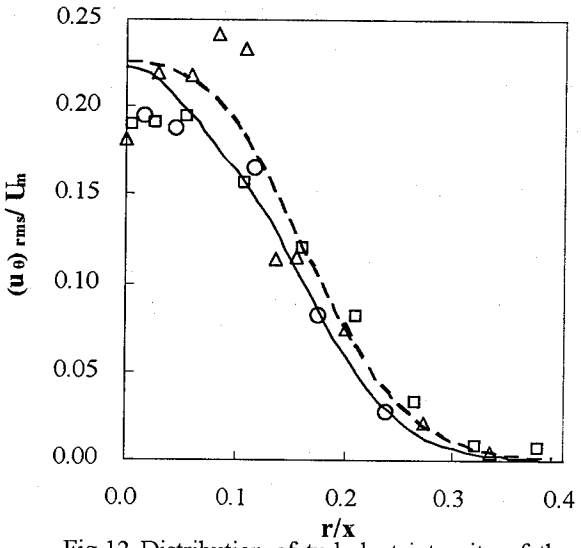

Fig.12 Distribution of turbulent intensity of the circumferential velocity in a swirl jet

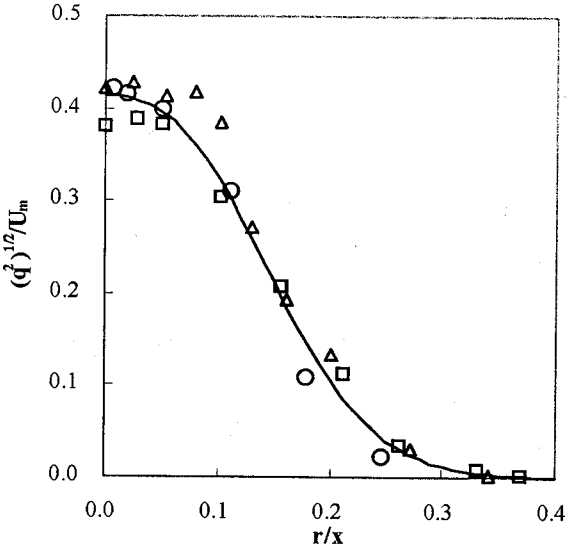

Fig.13 Radial distribution of turbulent kinetic energy in a swirl jet

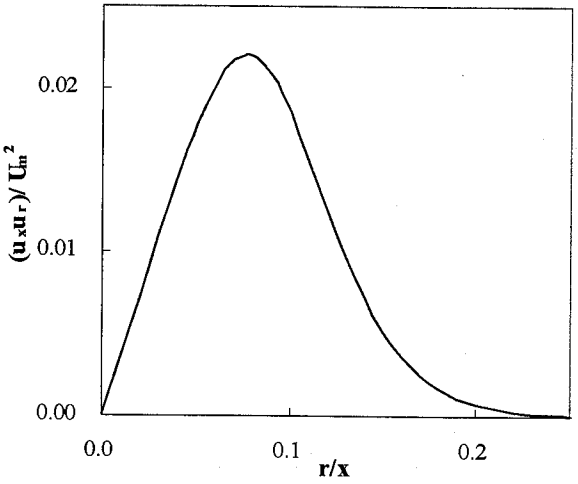

Fig.14 Radial distribution of turbulent shear stress in a swirl jet

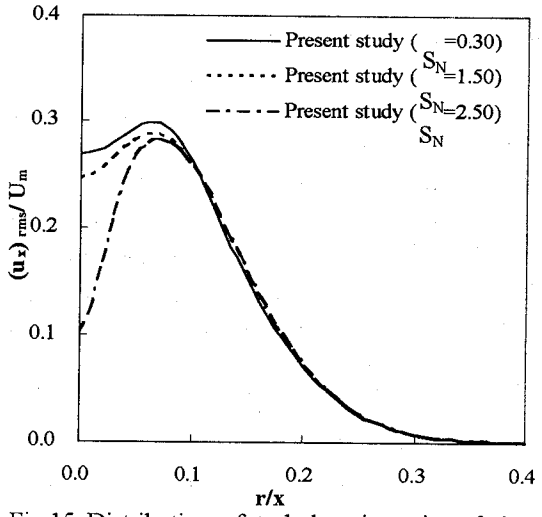

Fig.15 Distribution of turbulent intensity of the axial velocity for different swirl numbers

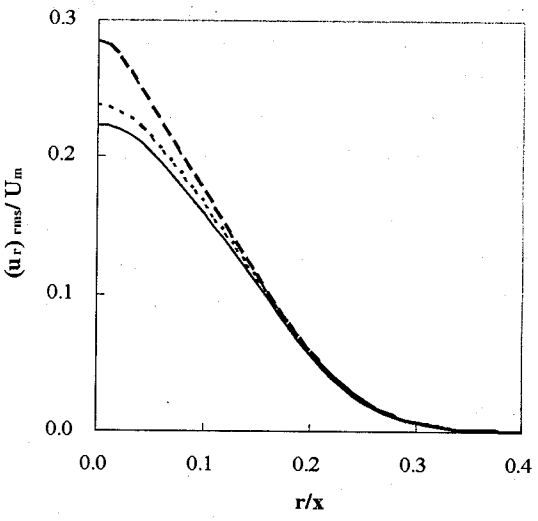

Fig.16 Distribution of turbulent intensity of the radial velocity for different swirl numbers

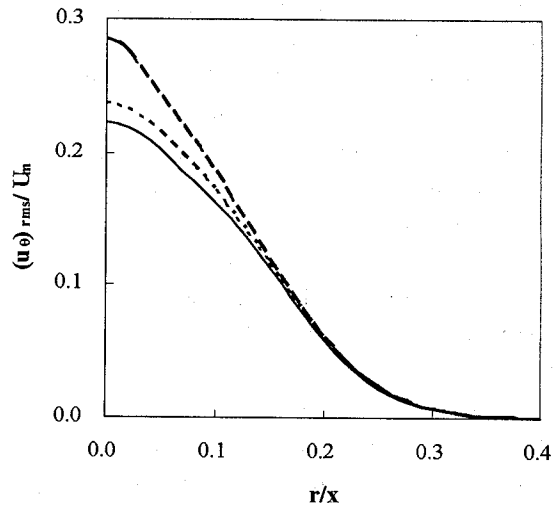

Fig.17 Distribution of turbulent intensity of the circumferential velocity for different swirl numbers

which is about 21% higher than the estimated half-width of a round jet without swirl. Gibson and Younis[6] also reported similar comparison with a difference of 25% between the jet-half width of swirl and non-swirl round jets.

The turbulent intensities for axial, lateral and circumferential velocities are calculated with the same swirl number. The results are compared with experimental data by Pratte and Keffer[5] in Figs. 10 to 12. The root-mean-square turbulent intensities and radial distance are normalized by centerline maximum velocity and the downstream distance respectively. The figurers show that the prediction of standard k–ε model is not as good as that of non-linear one.

In Fig. 13, the distribution of normalized turbulent kinetic energy $\left(\overline{q^2}\right)^{\frac{1}{2}}/U_m$ (where, $\overline{q^2}$ is twice the turbulent kinetic energy), is favorably compared with the previous experiment. Figure 14 shows the radial distribution of turbulent Reynolds stress $\overline{u_x u_r}$.

The distributions of turbulent intensities are found to be changed significantly depending on swirl number. For different swirl numbers of S_N = 0.3, 1.5 and 2.5, the turbulent intensities are calculated. The radial distributions of turbulent intensities for axial, radial and circumferential velocities are shown in Figs. 15, 16, and 17 respectively. It is observed that, with increasing swirl number the turbulent intensity is decreased for axial velocity component and increased for lateral and circumferential velocity components.

7. Conclusion

Based on a realizable non-linear k– ε model, approximate solutions for the fundamental properties of a swirl jet are derived. The functional forms of velocities as well as k and ε distributions are assumed as a first approximation. The unknown coefficients in the functional forms are obtained as the function of the non-linear $k-\varepsilon$ model constants by solving the continuity, momentum and non-linear $k-\varepsilon$ equations. The turbulent intensities and shear stresses are derived from a non-linear Reynolds stress equation. The coefficient of eddy viscosity (c_μ) is determined as a function of strain and rotation parameters, and the constraints of the functions are determined considering the realizability conditions for a simple shear layer problem.

Neglecting swirl parameter, the same solutions are applied for a round jet; and the calculated spreading rate, radial distribution of turbulent intensities, turbulent shear stress, turbulent kinetic energy and dissipation rate of turbulent kinetic energy are compared with the previous experimental results. A well agreed comparison to previous experiments revealed the performance of the present model.

For swirl jet, the calculated spreading rate and turbulent intensities are well agreed with the previous experiments. Through this comparison, the applicability of this model to estimate the fundamental properties of the swirl jet is verified. However, further studies are required to verify the applicability of this non-linear $k-\varepsilon$ model to various turbulent flows especially for large scale vortices.

Appendix-A: Derived Equations

Derived equations for the distributions of turbulent intensities in a swirl jet are given below.

$$\overline{u_x u_x} = \left\{2a_1 - \frac{r^2}{x^2}\left(\frac{4a_1}{\gamma^2} - \frac{6a_3}{\gamma^2}\right)\right\}\frac{c_\mu k'^2}{\varepsilon'}\frac{1}{x^2}\exp\left(-2\frac{r^2}{\gamma^2 x^2}\right)$$

$$+ c_\mu \frac{k'^3}{\varepsilon'^2}\frac{1}{x^2}\exp\left(-2\frac{r^2}{\gamma^2 x^2}\right)\times\left[(c_1+c_2+c_3)\left(\frac{2}{3}a_1{}^2 - \frac{2}{3}\frac{b^2}{\gamma^2}\right)\right.$$

$$-(c_1-c_2+c_3)\frac{1}{x^2}\left(\frac{2}{3}\frac{\alpha^2}{\gamma^2}\right)+\frac{r^2}{x^2}\left\langle c_1\left\{\frac{2}{3}\left(\frac{2a_3}{\gamma^2}-\frac{2a_1}{\gamma^2}\right)^2\right.\right.$$

$$-\frac{4}{3}\left(\frac{2a_1{}^2}{\gamma^2}-\frac{3a_1a_3}{\gamma^2}\right)-\frac{4}{3}\frac{b^2}{\gamma^2}+\frac{4}{3}\frac{b^2}{\gamma^4}+\frac{1}{x^2}\left(\frac{4}{3}\frac{\alpha^2}{\gamma^4}-\frac{3\alpha^2}{\gamma^2}\right)\Bigg\}$$

$$+c_2\left\{-\frac{4}{3}\left(\frac{2a_1{}^2}{\gamma^2}-\frac{3a_1a_3}{\gamma^2}\right)-\frac{2}{3}\frac{b}{\gamma}\left(\frac{2a_3}{\gamma^2}-\frac{2a_1}{\gamma^2}\right)+\frac{4}{3}\frac{b^2}{\gamma^4}-\frac{1}{x^2}\left(\frac{4}{3}\frac{\alpha^2}{\gamma^4}\right)\right\}$$

$$+c_3\left\{-\frac{1}{3}\left(\frac{2a_3}{\gamma^2}-\frac{2a_1}{\gamma^2}\right)^2-\frac{4}{3}\left(\frac{2a_1{}^2}{\gamma^2}-\frac{3a_1a_3}{\gamma^2}\right)+\frac{8}{3}\frac{b^2}{\gamma^2}+\frac{4}{3}\frac{b^2}{\gamma^4}\right.$$

$$\left.\left.+\frac{1}{x^2}\left(\frac{4}{3}\frac{\alpha^2}{\gamma^4}+\frac{6\alpha^2}{\gamma^2}\right)\right\}\right\rangle+\frac{r^4}{x^4}\left\langle c_1\left\{\frac{2}{3}\left(\frac{2a_1}{\gamma^2}-\frac{3a_3}{\gamma^2}\right)^2\right.\right.$$

$$-\frac{8}{3}\frac{a_3}{\gamma^4}\left(\frac{2a_3}{\gamma^2}-\frac{2a_1}{\gamma^2}\right)-\frac{4}{3}\frac{b^2}{\gamma^6}+\frac{8}{3}\frac{b^2}{\gamma^4}\Bigg\}+c_2\left\{\frac{2}{3}\left(\frac{2a_1}{\gamma^2}-\frac{3a_3}{\gamma^2}\right)^2\right.$$

$$+\frac{2}{3}\frac{b}{\gamma^3}\left(\frac{2a_3}{\gamma^2}-\frac{2a_1}{\gamma^2}\right)-\frac{4}{3}\frac{b^2}{\gamma^6}+\frac{4}{3}\frac{a_3 b}{\gamma^5}\Bigg\}+c_3\left\{\frac{2}{3}\left(\frac{2a_1}{\gamma^2}-\frac{3a_3}{\gamma^2}\right)^2\right.$$

$$\left.\left.\left.+\frac{4}{3}\frac{a_3}{\gamma^4}\left(\frac{2a_3}{\gamma^2}-\frac{2a_1}{\gamma^2}\right)-\frac{4}{3}\frac{b^2}{\gamma^6}-\frac{16}{3}\frac{b^2}{\gamma^4}\right\}\right\rangle\right]$$

$$+\frac{2}{3}\frac{1}{x^2}\left(k_0+k_2\frac{r^2}{\gamma^2 x^2}\right)\exp\left(-2\frac{r^2}{\gamma^2 x^2}\right) \qquad \text{(A1)}$$

$$\overline{u_r u_r} = \left\{-2\frac{b}{\gamma}+\frac{4b}{\gamma^3}\frac{r^2}{x^2}\right\}c_\mu\frac{k'^2}{\varepsilon'}\frac{1}{x^2}\exp\left(-2\frac{r^2}{\gamma^2 x^2}\right)$$

$$+c_\mu\frac{k'^3}{\varepsilon'^2}\frac{1}{x^2}\exp\left(-2\frac{r^2}{\gamma^2 x^2}\right)\times\left[(c_1+c_2+c_3)\left(\frac{1}{3}\frac{b^2}{\gamma^2}-\frac{1}{3}a_1{}^2\right)\right.$$

$$+(c_1-c_2+c_3)\frac{1}{x^2}\left(\frac{1}{3}\frac{\alpha^2}{\gamma^2}\right)+\frac{r^2}{x^2}\left\langle c_1\left\{-\frac{1}{3}\left(\frac{2a_3}{\gamma^2}-\frac{2a_1}{\gamma^2}\right)^2\right.\right.$$

$$+\frac{2}{3}\left(\frac{2a_1^2}{\gamma^2}-\frac{3a_1a_3}{\gamma^2}\right)-\frac{4}{3}\frac{b^2}{\gamma^2}+\frac{4}{3}\frac{b^2}{\gamma^4}+\frac{1}{x^2}\left(\frac{4}{3}\frac{\alpha^2}{\gamma^4}-\frac{3\alpha^2}{\gamma^2}\right)\Bigg\}$$

$$+c_2\left\{\frac{2}{3}\left(\frac{2a_1^2}{\gamma^2}-\frac{3a_1a_3}{\gamma^2}\right)+\frac{4}{3}\frac{b}{\gamma}\left(\frac{2a_3}{\gamma^2}-\frac{2a_1}{\gamma^2}\right)+\frac{4}{3}\frac{b^2}{\gamma^4}-\frac{4}{3}\frac{b^2}{\gamma^2}\right\}$$

$$+\frac{1}{x^2}\left(\frac{2}{3}\frac{\alpha^2}{\gamma^4}\right)+c_3\left\{-\frac{1}{3}\left(\frac{2a_3}{\gamma^2}-\frac{2a_1}{\gamma^2}\right)^2+\frac{2}{3}\left(\frac{2a_1^2}{\gamma^2}-\frac{3a_1a_3}{\gamma^2}\right)\right.$$

$$\left.-\frac{4}{3}\frac{b^2}{\gamma^2}+\frac{4}{3}\frac{b^2}{\gamma^4}-\frac{1}{x^2}\left(\frac{8}{3}\frac{\alpha^2}{\gamma^4}+\frac{3\alpha^2}{\gamma^2}\right)\right\}\Bigg\rangle+\frac{r^2}{x^2}\Bigg\langle c_1\left\{4\frac{b^2}{\gamma^2}-4\frac{b^2}{\gamma^4}\right\}$$

$$+c_2\left\{-2\frac{b}{\gamma}\left(\frac{2a_3}{\gamma^2}-\frac{2a_1}{\gamma^2}\right)-4\frac{b^2}{\gamma^4}\right\}+c_3\left\{\left(\frac{2a_3}{\gamma^2}-\frac{2a_1}{\gamma^2}\right)^2-4\frac{b^2}{\gamma^4}\right\}\Bigg\rangle$$

$$+\frac{r^4}{x^4}\Bigg\langle c_1\left\{-\frac{1}{3}\left(\frac{2a_1}{\gamma^2}-\frac{3a_3}{\gamma^2}\right)^2+\frac{4}{3}\frac{a_3}{\gamma^4}\left(\frac{2a_3}{\gamma^2}-\frac{2a_1}{\gamma^2}\right)-\frac{4}{3}\frac{b^2}{\gamma^6}+\frac{8}{3}\frac{b^2}{\gamma^4}\right\}$$

$$+c_2\left\{-\frac{1}{3}\left(\frac{2a_1}{\gamma^2}-\frac{3a_3}{\gamma^2}\right)^2-\frac{2}{3}\frac{b}{\gamma^3}\left(\frac{2a_3}{\gamma^2}-\frac{2a_1}{\gamma^2}\right)-\frac{8}{3}\frac{a_3b}{\gamma^5}\right\}$$

$$+c_3\left\{-\frac{1}{3}\left(\frac{2a_1}{\gamma^2}-\frac{3a_3}{\gamma^2}\right)^2+\frac{4}{3}\frac{a_3}{\gamma^4}\left(\frac{2a_3}{\gamma^2}-\frac{2a_1}{\gamma^2}\right)-\frac{4}{3}\frac{b^2}{\gamma^6}+\frac{8}{3}\frac{b^2}{\gamma^4}\right\}\Bigg\rangle\Bigg]$$

$$+\frac{r^4}{x^4}\Bigg\langle c_1\left\{4\frac{b^2}{\gamma^6}-8\frac{b^2}{\gamma^4}\right\}+c_2\left\{2\frac{b}{\gamma}\left(\frac{4a_3}{\gamma^4}-\frac{2a_1}{\gamma^4}\right)+4\frac{b^2}{\gamma^6}\right\}$$

$$+c_3\left\{-\frac{4a_3}{\gamma^4}\left(\frac{2a_3}{\gamma^2}-\frac{2a_1}{\gamma^2}\right)+4\frac{b^2}{\gamma^6}\right\}\Bigg\rangle$$

$$+\frac{2}{3}\frac{1}{x^2}\left(k_0+k_2\frac{r^2}{\gamma^2x^2}\right)\exp\left(-2\frac{r^2}{\gamma^2x^2}\right) \qquad \text{(A2)}$$

$$\overline{u_\theta u_\theta}=\left\{-2\frac{b}{\gamma}\right\}c_\mu\frac{k'^2}{\varepsilon'}\frac{1}{x^2}\exp\left(-2\frac{r^2}{\gamma^2x^2}\right)$$

$$+c_\mu\frac{k'^3}{\varepsilon'^2}\frac{1}{x^2}\exp\left(-2\frac{r^2}{\gamma^2x^2}\right)\times\Bigg[(c_1+c_2+c_3)\left(\frac{1}{3}\frac{b^2}{\gamma^2}-\frac{1}{3}a_1^2\right)$$

$$+(c_1-c_2+c_3)\frac{1}{x^2}\left(\frac{1}{3}\frac{\alpha^2}{\gamma^2}\right)+\frac{r^2}{x^2}\Bigg\langle c_1\left\{-\frac{1}{3}\left(\frac{2a_3}{\gamma^2}-\frac{2a_1}{\gamma^2}\right)^2\right.$$

$$\left.+\frac{2}{3}\left(\frac{2a_1^2}{\gamma^2}-\frac{3a_1a_3}{\gamma^2}\right)-\frac{4}{3}\frac{b^2}{\gamma^2}+\frac{4}{3}\frac{b^2}{\gamma^4}+\frac{1}{x^2}\left(\frac{4}{3}\frac{\alpha^2}{\gamma^4}-\frac{3\alpha^2}{\gamma^2}\right)\right\}$$

$$+c_2\left\{\frac{2}{3}\left(\frac{2a_1^2}{\gamma^2}-\frac{3a_1a_3}{\gamma^2}\right)+\frac{4}{3}\frac{b}{\gamma}\left(\frac{2a_3}{\gamma^2}-\frac{2a_1}{\gamma^2}\right)+\frac{4}{3}\frac{b^2}{\gamma^4}-\frac{4}{3}\frac{b^2}{\gamma^2}\right\}$$

$$+\frac{1}{x^2}\left(\frac{2}{3}\frac{\alpha^2}{\gamma^4}\right)+c_3\left\{-\frac{1}{3}\left(\frac{2a_3}{\gamma^2}-\frac{2a_1}{\gamma^2}\right)^2+\frac{2}{3}\left(\frac{2a_1^2}{\gamma^2}-\frac{3a_1a_3}{\gamma^2}\right)\right.$$

$$\left.-\frac{4}{3}\frac{b^2}{\gamma^2}+\frac{4}{3}\frac{b^2}{\gamma^4}-\frac{1}{x^2}\left(\frac{8}{3}\frac{\alpha^2}{\gamma^4}+\frac{3\alpha^2}{\gamma^2}\right)\right\}\Bigg\rangle$$

$$+\frac{r^4}{x^4}\Bigg\langle c_1\left\{-\frac{1}{3}\left(\frac{2a_1}{\gamma^2}-\frac{3a_3}{\gamma^2}\right)^2+\frac{4}{3}\frac{a_3}{\gamma^4}\left(\frac{2a_3}{\gamma^2}-\frac{2a_1}{\gamma^2}\right)-\frac{4}{3}\frac{b^2}{\gamma^6}+\frac{8}{3}\frac{b^2}{\gamma^4}\right\}$$

$$+c_2\left\{-\frac{1}{3}\left(\frac{2a_1}{\gamma^2}-\frac{3a_3}{\gamma^2}\right)^2-\frac{2}{3}\frac{b}{\gamma^3}\left(\frac{2a_3}{\gamma^2}-\frac{2a_1}{\gamma^2}\right)-\frac{8}{3}\frac{a_3b}{\gamma^5}\right\}$$

$$+c_3\left\{-\frac{1}{3}\left(\frac{2a_1}{\gamma^2}-\frac{3a_3}{\gamma^2}\right)^2+\frac{4}{3}\frac{a_3}{\gamma^4}\left(\frac{2a_3}{\gamma^2}-\frac{2a_1}{\gamma^2}\right)-\frac{4}{3}\frac{b^2}{\gamma^6}\right.$$

$$\left.+\frac{8}{3}\frac{b^2}{\gamma^4}\right\}\Bigg\rangle\Bigg]+\frac{2}{3}\frac{1}{x^2}\left(k_0+k_2\frac{r^2}{\gamma^2x^2}\right)\exp\left(-2\frac{r^2}{\gamma^2x^2}\right) \qquad \text{(A3)}$$

The derived equation for the turbulent shear stress is as follows.

$$\overline{u_xu_r}=\left\{\left(\frac{2a_1}{\gamma^2}-\frac{2a_3}{\gamma^2}+\frac{3b}{2\gamma}\right)\frac{r}{x}\right\}c_\mu\frac{k'^2}{\varepsilon'}\frac{1}{x^2}\exp\left(-2\frac{r^2}{\gamma^2x^2}\right)$$

$$+c_\mu\frac{k'^3}{\varepsilon'^2}\frac{1}{x^2}\exp\left(-2\frac{r^2}{\gamma^2x^2}\right)\times\Bigg[\frac{r}{x}\Bigg\langle c_1\left\{\frac{b}{\gamma}\left(\frac{2a_3}{\gamma^2}-\frac{2a_1}{\gamma^2}+2a_1\right)\right.$$

$$\left.+c_2\left\{\frac{1}{2}\frac{b}{\gamma}\left(\frac{2a_3}{\gamma^2}-\frac{2a_1}{\gamma^2}\right)+\frac{a_1b}{\gamma}-\frac{a_1}{2}\left(\frac{2a_3}{\gamma^2}-\frac{2a_1}{\gamma^2}\right)-\frac{b^2}{\gamma^2}+\left(\frac{3}{2}\frac{\alpha^2}{x^2\gamma^2}\right)\right\}\right.$$

$$\left.+c_3\left\{-a_1\left(\frac{2a_3}{\gamma^2}-\frac{2a_1}{\gamma^2}\right)-2\frac{b^2}{\gamma^2}-3\frac{\alpha^2}{x^2\gamma^2}\right\}\Bigg\rangle\right.$$

$$+\frac{r^3}{x^3}\Bigg\langle c_1\left\{-2\frac{b}{\gamma}\left(\frac{3a_1}{\gamma^2}-\frac{3a_3}{\gamma^2}\right)-\frac{2a_3b}{\gamma^5}-2\frac{b}{\gamma^3}\left(\frac{2a_3}{\gamma^2}-\frac{2a_1}{\gamma^2}\right)\right\}$$

$$+c_2\left\{-\frac{b}{\gamma}\left(\frac{2a_1}{\gamma^2}-3\frac{a_3}{\gamma^2}\right)-\frac{a_1b}{\gamma}-\frac{b}{\gamma^3}\left(\frac{2a_3}{\gamma^2}-\frac{2a_1}{\gamma^2}\right)\right.$$

$$\left.+\frac{1}{2}\left(\frac{2a_1}{\gamma^2}-\frac{3a_3}{\gamma^2}\right)\left(\frac{2a_3}{\gamma^2}-\frac{2a_1}{\gamma^2}\right)+\frac{a_1a_3}{\gamma^4}+\frac{3b^2}{\gamma^4}\right\}$$

$$+c_3\left\{\left(\frac{2a_1}{\gamma^2}-\frac{3a_3}{\gamma^2}\right)\left(\frac{2a_3}{\gamma^2}-\frac{2a_1}{\gamma^2}\right)+\frac{2a_1a_3}{\gamma^4}+\frac{2b^2}{\gamma^4}\right\}\Bigg\rangle\Bigg] \qquad \text{(A4)}$$

Here, $\varepsilon'=\left(\varepsilon_0+\varepsilon_2\frac{r^2}{\gamma^2x^2}\right)$ and $k'=\left(k_0+k_2\frac{r^2}{\gamma^2x^2}\right)$

Appendix-B: Notation of Symbols

A_0 = area of the jet at inlet

a_1, a_3, b = coefficients of the assumed velocity profiles

B = jet width

$c_{\varepsilon1}$, $c_{\varepsilon2}$ = $k-\varepsilon$ model constants

c_μ, c_β (c_1, c_2, c_3) = non-linear $k-\varepsilon$ model constants

$c_{\mu0}$, c_{ns}, $c_{n\Omega}$, c_{ds}, $c_{d\Omega}$, $c_{ds\Omega}$, c_{ds1}, $c_{d\Omega1}$, $c_{ds\Omega1}$ = model

constants for c_μ

$c_{\beta 0}$ = the model constants for c_β

k = turbulent energy

k_0, k_2 = coefficients of the assumed k distribution

M_0 = initial momentum flux of the jet

$m_{ns}, m_{n\Omega}, m_{ds}, m_{d\Omega}$= model constants for c_β

P = pressure

r_0 =radius of the jet nozzle

$r_{1/2}$ = jet half-width

S = strain parameter defined by Eq. (15)

S_N =swirl number

S_{ij} = strain rate tensors

U_0 = velocity of the jet at inlet

U_m = centerline maximum velocity of the jet

U_i = average velocity in x_i direction

U_x, U_y, U_z =velocities in Cartesian coordinate system

U_x, U_r, U_θ = velocities in Cylindrical coordinate system

u_i = turbulent velocity in x_i direction

$\overline{u_i u_j}$ = Reynolds stress tensor

x_i =spatial coordinates

x, y, z = axial, lateral, and transverse directions in Cartesian coordinate system

x, r, θ= axial, radial and azimuthal directions in Cylindrical coordinate system

α, γ = coefficients of the assumed velocity profiles

ε = turbulent energy dissipation rate

$\varepsilon_0, \varepsilon_2$ = coefficients of the assumed ε distribution

ρ = density of fluid

ν = molecular dynamic viscosity

ν_t = eddy viscosity

$\sigma_k, \sigma_\varepsilon$ = $k-\varepsilon$ model constants

Ω = rotation parameter defined by Eq. (15)

Ω_{ij} = rotation rate tensor

References

1) Panda, J. and Mclaughin, D. K., Experiments in the instabilities of a swirling jet, *Phys. Fluids.* 6, pp.263-276, 1994.

2) Billiant, P., Chomaz J. M., Huerre, P., Experimenttal study of vortex breakdown in swirling jet, *J. Fluid Mech.* 376, pp.183-219, 1998.

3) Ribeiro, M. M. and Whitelaw, J. H., Coaxial jets with and without swirl, *J. Fluid Mech.* 96, pp.769-795, 1980.

4) Paschereit, C. O., Gutmark, K. E. and Weisenstein, W., Coherent structures in swirling flows and their role in acoustic combustion control, *Phys. Fluids.* 11, pp.2667, 1999.

5) Pratte, B. D. and Keffer, J. F., The swirling turbulent jet, *J. Basic Engg., Trans. ASME*, pp. 739-748, 1972.

6) Gibson, M. M. and Younis, B. A., Calculation of swirling jets with a Reynolds stress model, *Phys. Fluids.* 29, pp.38-48, 1986.

7) Mcllwain, S. and Pollard, A., Large eddy simulation of the effects of mild swirl on the near field of a round free jet, *Phys. Fluids.* 14, pp.653-661, 2002.

8) Wang, P., Bai, X. S., Wessman. M. and Klingmann, J., Large eddy simulation and experimental studies of a turbulent swirling jet, *Phys. Fluids.* 16, pp.3303-3324, 2004.

9) Jaw, S.Y. and Chen, C. J., Present status of second order closure turbulence models. I: overview, *J. Engg. Mech., ASCE.* 124, pp.485-501, 1998.

10) Rodi, W., Turbulence models for environmental problems, in *Prediction methods for turbulent flows (edited by W. Kollmann)*, pp.259, 1979.

11) Yoshizawa, A., Statistical analysis of the deviation of the Reynolds stress from its eddy viscosity representation, *Phys. Fluids*, 27, pp.1377-1387, 1984.

12) Pope, S. B., A more general effective viscosity hypothesis, *J. Fluid Mech.* 72, pp.331-340, 1975.

13) Gatski, T. B. and Speziale, C. G., On explicit algebraic stress models for complex turbulent flows, *J. Fluid Mech.* 254, pp.59-78, 1993.

14) Kimura, I. and Hosoda, T., A non-linear k - ϵ model with realizability for prediction of flows around bluff bodies, *Int. J. Numer. Meth. Fluids.* 42, pp.813-837, 2003.

15) Shih,T. H., Zhu, J. and Lumley, J. L., Calculation of bounded complex flows and free shear flows, *Int. J. Numer. Meth. Fluids.* 33, pp.1133-1144, 1996.

16) Hosoda, T., Iwasa, Y. and Yokosi, S., Hydraulic analysis of turbulent jets by means of k - ε models, *Research Report no. 84-HY-01, School of Civil Engineering, Kyoto University, Japan*, 1984.

17) Rajaratnam, N., *Turbulent jets*, Elsevier scientific publishing company, 1976.

18) Wygnanski, I. and Fielder, H., Some measurements in the self-preserving jet, *J. Fluid Mech.* 38, pp.577-612 (1969).

19) Wang, H. and Law, A. W. K., Second-order integral model for a round turbulent jet, *J. Fluid Mech.* 459, pp.397-428, 2002.

20) Fukushima, C., Aanen, L. and Westerweel, J., Investigation of the mixing process in an axisymmetric turbulent jet using PIV and LIF, *Proc. Int. Symp. on application of laser techniques to fluid mechanics (Lisbon, Portugal)*, paper 11.1, July 10-13, 2000.

21) Sami, S., Balance of turbulence energy in the region of jet flow establishment, *J. Fluid. Mech.* 29, pp.81-92, 1967.

22) Rose, W. G., A swirling round turbulent jet, *J. Appl. Mech., Trans. ASME*, 29, pp.615-625, 1962.

(Received: April 13, 2006)